A molecular dynamics simulation study on solubility behaviors of polycyclic aromatic hydrocarbons in supercritical water/hydrogen environment

Weijing Ding, Jinwen Shi, Wenwen Wei, Changqing Cao, Hui Jin[*]

State Key Laboratory of Multiphase Flow in Power Engineering, Xi'an JiaoTong University, Xi'an, 710049, Shaanxi, China

HIGHLIGHTS

- Solubility of PAHs in SCW/H_2 was studied by MD simulations.
- Increasing temperature and density enhanced solubility behaviors.
- It was observed that hydrogen penetrated water shells.
- Hydrogen promoted the dispersion of PAH oil droplets.

GRAPHICAL ABSTRACT

ARTICLE INFO
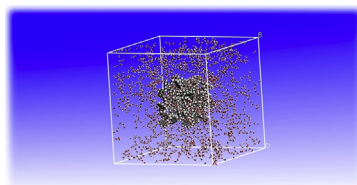
ABSTRACT

Violates containing polycyclic aromatic hydrocarbons (PAHs) were precipitated in the process of fast pyrolysis and gasification of coal and organic substances. PAHs are one of bottlenecks of entire coal gasification for hydrogen production. In current work, the solubility of PAH oil droplets in supercritical water/hydrogen circumstances were investigated based on molecular dynamics simulation, which was beneficial for understanding the solubility behaviors of PAHs in supercritical water/hydrogen environment. The results showed that heavy PAHs were rather stable in the water phase. Supercritical water along with hydrogen promoted the miscibility of PAHs compared with that of pure supercritical water. Furthermore, high density and high temperature facilitated the rapid solvation of PAHs in supercritical water/hydrogen environment. This paper is expected to provide a theoretical support for the development of complete coal gasification technology for hydrogen production.

Introduction

Coal, as one of fossil resources, still takes an important part in energy structure, extremely in the winter heating period of cold areas. Direct combustion of coal causes severe environmental pollution, especially CO_2 emission [1—3]. Thus, how to achieve clean and efficient utilization of coal is a crucial topic of scientific research. Notably, coal and biomass can react with water to produce hydrogen [4—6]. Hydrogen could be used for clean combustion, heating, power generation and energy storage. Especially, supercritical water (SCW, temperature > 647.4 K and pressure > 22.1 MPa) [7—9] gasification for hydrogen production is an ideal approach of efficient and clean utilization of fossil fuels [10,11]. Supercritical water gasification of coal [10,11] or organic wastes [12—15], as a clean and efficient approach of energy utilization, has very broad application aspects and prospects in the future. However, there are some problems, such as coke formation, low carbon conversion, and the decomposition and conversion of polycyclic aromatic hydrocarbons (PAHs) and other macromolecular compounds. The internal mechanism in complex molecular system is urged to be further explored, which is conducive to promoting the efficient and clean utilization of energy and sustainable development. Notably, molecular simulation can be adopted to study intrinsic mechanisms in the process of hydrogen production from coal gasification, such as the pyrolysis and gasification mechanism of coal [16—18], PAHs [19] and other molecular model compounds [12,20], which can provide a theoretical basis for the development and industrialization of hydrogen production.

Molecular dynamics (MD)simulation can be applied to illustrate and reveal internal behaviors and mechanisms on molecular scale in complex molecular system [19,21], which is one of theoretical computation approaches. Numerical studies [22,23] also have been used. Researchers had studied the diffusion properties of gases in supercritical water based on MD simulation. For instance, the diffusion behavior of carbon dioxide in supercritical water was simulated by Cai et al. [24,25]. The results manifested that the diffusion coefficient increased with temperature, whereas it decreased with pressure [24,25]. Actually, the varying temperature and pressure directly bear on the parameters of supercritical stream, involving density, viscosity as well as thermal conductivity [26]. For oxygen diffusion in supercritical water, there were few reports on account of experimental constraint; extremely the Darken equation was not valid for oxygen diffusion in supercritical water [27]. For hydrogen diffusion in supercritical water, Zhao et al. [28—30] obtained the diffusion properties under different statuses. Diffusion coefficients and correlations of various solutes in water at supercritical state have been estimated and calculated. Moreover, it was speculated that high diffusivity of reactants was a crucial factor, which is responsible for high degradation efficiency of oxidation reactions [31,32] in supercritical water. In addition, violates containing PAHs precipitate in the process of fast pyrolysis of coal and organic substances. PAHs have become one of bottlenecks in complete coal conversion for generating hydrogen [19,33]. Ever since Modell put forward SCW gasification [34] for hydrogen production, this technology has been dramatically developed. SCW gasification can not just improve the utilization efficiency of fossil fuels and organic wastes [35,36], but reduce environmental pollution [37—40]. Dissolution of PAHs and mixtures [41—43] in water at supercritical state had been explored and studied. It was revealed that supercritical water has great solubility abilities for organic substances including PAHs, which deserves extensive investigations [41—44]. In this article, MD calculations were applied to investigate the miscibility of PAHs with supercritical water/hydrogen for illustrating solubility behaviors and structures in the solvent. This work is willing to offer a theoretical support for the development of entire coal gasification technology for hydrogen production, which is conducive to prompting the sustainable development of energy and environment.

Simulation details and verifications

Naphthalene (NAP) was adopted as light PAHs in current work, while benzo [ghi]perylene (Bghip) were selected as heavy PAHs. The reliability of a MD simulation primarily depends on the force field applied. The validity of COMPASS in the hydrocarbons/SCW environment had been verified [45—47]. The non-bonding interaction between particles was described by COMPASS force field in this paper. For simulations, a cubic box with periodic boundaries was established to simulate the environment at supercritical state. An oil droplet containing PAH molecules was located at the center of the box in MD simulations. The left space of the box was full of water molecules. Water densities were ranging from 0.1 g/cm^3 to 0.3 g/cm^3 and relevant details were illustrated in Table 1. The whole calculations were based on a molecular dynamics module Forcite integrated in the software package of Materials Studio (Accelrys Inc.), which ran on the Dell Precision WorkStation T7500 Tower. Radial distribution function [41] (RDF) was obtained by the Forcite trajectory files.

Recorded. As shown in Fig. 1, the broadened peak of the RDF between oxygen atoms contained in water was 5.2 Å and the intensity of the peak declined, which was in line with the former reports [41] verifying the simulations. A typical molecular dynamics simulation on the dissolution of PAHs is illuminated as bellows. First, the bulk phase of PAHs was constructed and the stable bulk structure of PAHs was obtained by an anneal operation based on NPT ensemble. Based on the research, an oil droplet about 15 Å in radius containing 60 wt% Bghip (weight ratio) and 40 wt% NAP ($Bghip_{60}NAP_{40}$) was acquired from the bulk phase and placed at the center of a cubic box 80 Å on every edge. When the dissolution was applied in hydrogen and supercritical water solvent, 254 hydrogen molecules were contained [1,43]. Furthermore, the

Table 1 — System of PAHs solubility in SCW/hydrogen environment.

System	Number of water molecules	Hydrogen content (vol%)
PAHs-SCW/ hydrogen	1713	13.00
	3426	6.97
	5139	4.76
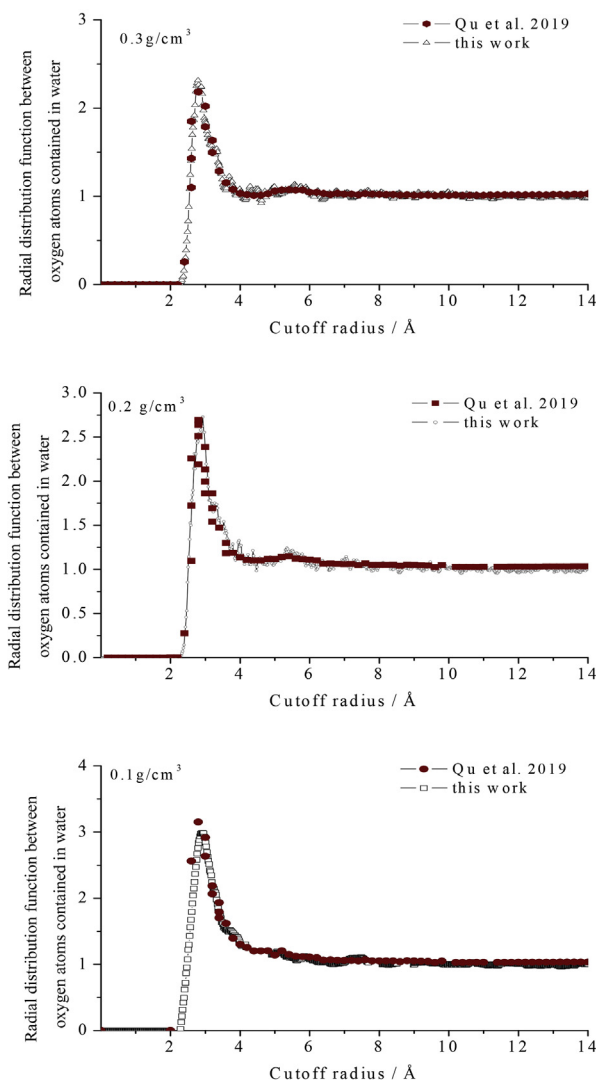
Fig. 1 – Radial distribution function curve of water at 683 K.

(a)Bghip₆₀NAP₄₀-0 ps

(b)Bghip₆₀NAP₄₀-125 ps

(c)Bghip₆₀NAP₄₀-375 ps

(d)Bghip₆₀NAP₄₀-500 ps

(e)Bghip₆₀NAP₄₀-125 ps

(f)Bghip₆₀NAP₄₀-170 ps

● ● ● C H O

Fig. 2 – Solubility of PAHs in solvent ●●● C H O. (a) ~ (d) SCW; (e) ~ (f) SCW/Hydrogen.

box was filled with water molecules whose density was adjusted by the number of water molecules, as mentioned above. Later, a MD simulation was conducted based on NVT ensemble and lasting 500 ps Besides, the atom based and Ewald summation methods were chosen for van der Waals and electrostatic, respectively. During the theoretical calculations, temperature oscillation was regulated by NHL thermostat.

Results and discussions

PAHs solubility behaviors in pure SCW and SCW/Hydrogen circumstances

The solubility of PAH (Bghip₆₀NAP₄₀) oil droplets in pure SCW and SCW/hydrogen circumstances was applied at the water density of 0.1 g/cm³ and the temperature of 683 K, as shown in Fig. 2.

At the time of 125 ps, light NAP molecules were evidently dissolved in supercritical water, while Bghip molecules were
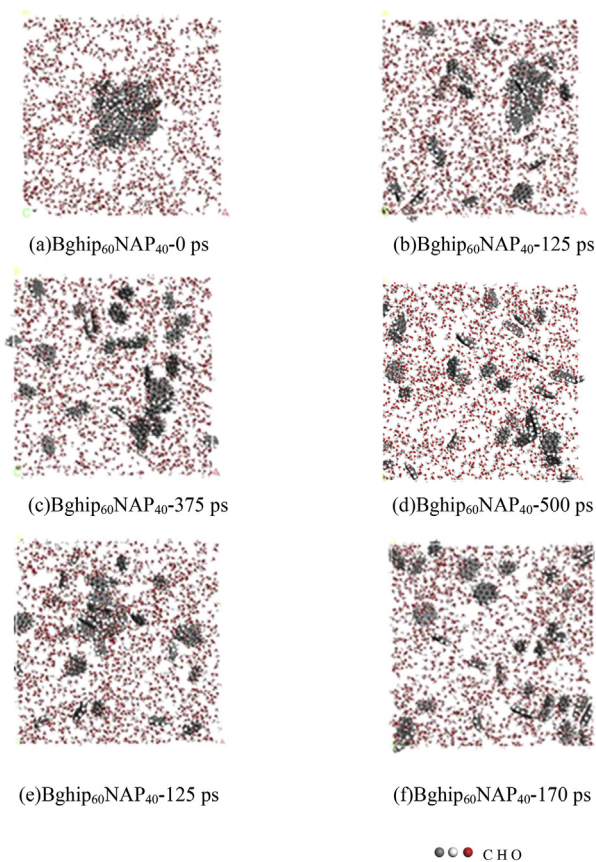
rather stable and remained in oil droplets, as observed in Fig. 2 (a)–(c). It was confirmed that heavy PAH molecules were more difficult to be dissolved than light ones in supercritical water [41–43]. The oil droplet was gradually dissolved in water phase with the time increasing. And the droplet was dramatically dissolved in water when the time reached 500 ps It was also found that nanoaggregates occurred during the simulations, which was primarily resulted from face-to-face, π-offset and T-shaped stacking among aromatic molecules [41,47]. Beside, compared with pure water, the PAHs dissolution was much quicker in supercritical water/hydrogen environment, as displayed in Fig. 2 (e)–(f). And the oil droplet was basically dissolved at 170 ps, which was even more significant than that of pure water at 375 ps It was revealed that the existence of hydrogen promoted the dispersion of PAH aggregates.

Furthermore, the miscibility of oil droplet (Bghip₆₀NAP₄₀) with supercritical water/hydrogen was applied at the water density of 0.2 g/cm³, as seen in Fig. 3. The oil droplet was immediately dispersed with time increasing. It was revealed in the previous studies [48] that supercritical water clusters provided OH and H free radicals, which greatly enhanced the production of carbon monoxide and hydrogen. According to Fig. 3 (a)–(c), water clusters and shells were surrounding with the oil droplet, which was in accordance with preceding reports [43,48] and this is essential to facilitate hydrogen generation [19,48] and production.
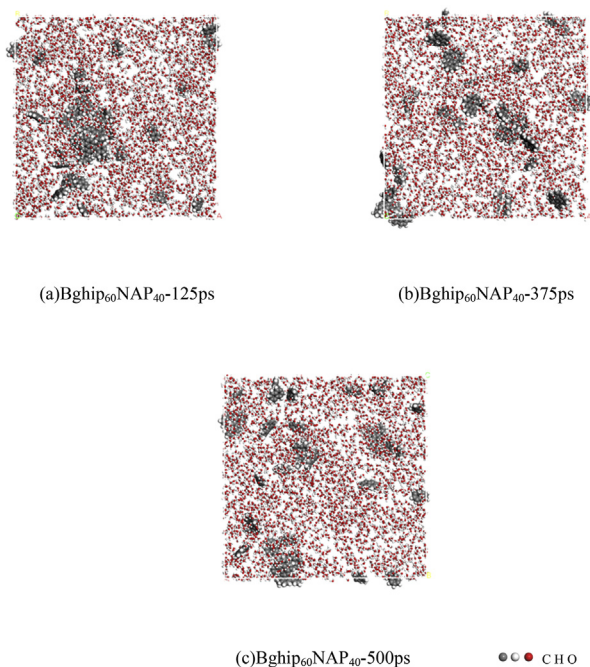
(a)Bghip$_{60}$NAP$_{40}$-125ps

(b)Bghip$_{60}$NAP$_{40}$-375ps

(c)Bghip$_{60}$NAP$_{40}$-500ps   ●◎● C H O

Fig. 3 – Dissolution on PAHs (Bghip$_{60}$NAP$_{40}$) in SCW/ Hydrogen environment.

PAH solubility behaviors at various hydrogen contents

The dissolution of PAHs (Bghip$_{60}$NAP$_{40}$) in supercritical water and hydrogen was applied at various hydrogen contents. Simultaneously, the temperature was fixed at 683 K. Then, at the simulation time of 125 ps, the PAHs solubility structures were as exhibited in Fig. 4. The results showed that solubility behaviors and dissolution structures were different under the three conditions. The solvation effect was the most significant
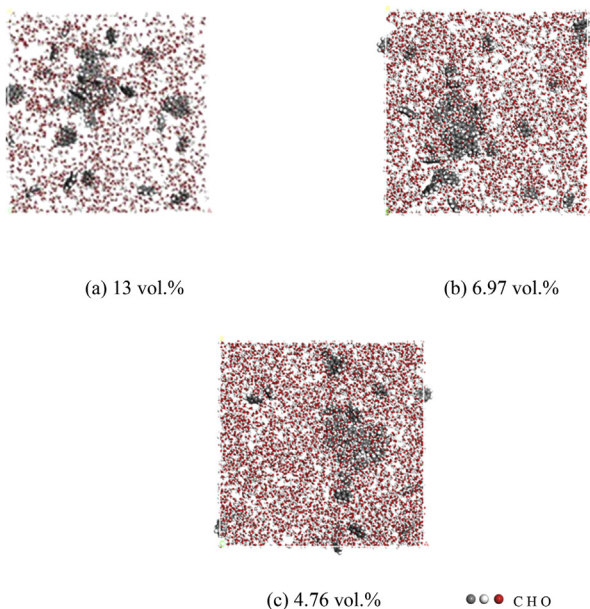
and evident at the time of 125 ps and the hydrogen content of 13 vol% (volume ratio). And the hydrogen pierced through water shells or clusters and prompted the dispersion of oil droplets.

Furthermore, the solubility and structure of PAHs (Bghip$_{60}$NAP$_{40}$) in supercritical water/hydrogen separately at 125 ps and 500 ps were illustrated in Fig. 5. According to Fig. 5 (a) and Fig.5 (b), Bghip molecules were not easy to be dissolved into the supercritical solvent. The scale of oil droplet decreased with the growth of time, as demonstrated in Fig. 5 (c) and Fig. 5 (d). Compared Fig. 5 (b) with Fig. 5 (d), the solubility performance at the density of 0.2 g/cm^3 was better than that of 0.1 g/cm^3. It is observed that a small droplet still exists in the solvent box in Fig. 5 (b), while in Fig. 5 (d) only PAH monomers and aggregates could be found in the solvent.

PAHs solubility behaviors under various temperatures

At after 125 ps, the oil droplet (Bghip$_{60}$NAP$_{40}$) solvation and structure in supercritical water/hydrogen under the condition of various temperatures were shown in Fig. 6. The water density was 0.3 g/cm^3 and the temperature was respectively 653 K, 683 K and 713 K.

As observed in Fig. 6, several PAH molecules had been dissolved into water phase at after 125 ps Moreover, the increase in temperature improved the dissolution ability on PAHs, which was in accordance with the results of previous reports [41–43]. By comparison, higher temperature has a positive impact on the PAHs solubility in supercritical water and hydrogen circumstances, as demonstrated in Fig. 6

(a) 13 vol.%

(b) 6.97 vol.%

(c) 4.76 vol.%   ●◎● C H O

Fig. 4 – Miscibility of PAHs (Bghip$_{60}$NAP$_{40}$) with SCW/ Hydrogen at different hydrogen contents.

(a) 125 ps-0.1g/cm^3

(b) 500 ps-0.1g/cm^3

(c) 125 ps-0.2g/cm^3

(d) 500 ps-0.2g/cm^3

●◎● C H O
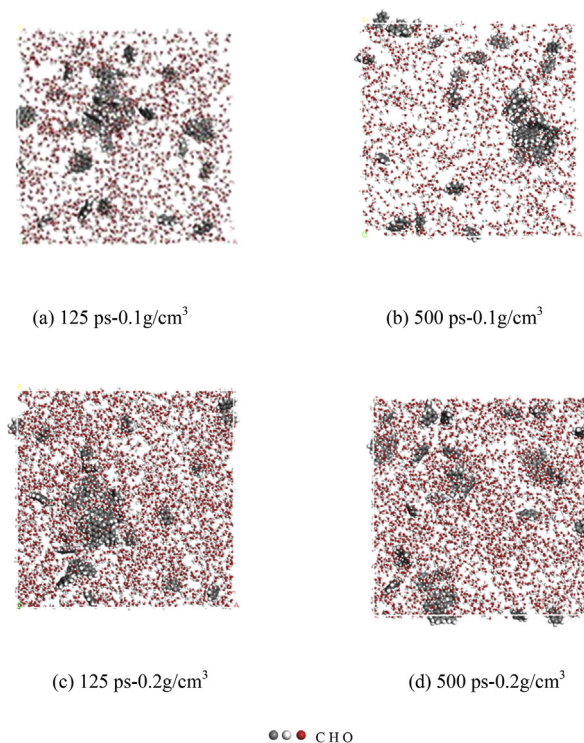
Fig. 5 – Solubility of PAHs (Bghip$_{60}$NAP$_{40}$) in SCW/ Hydrogen solvent.

(a)Bghip$_{60}$NAP$_{40}$ -653K　　　(b)Bghip$_{60}$NAP$_{40}$ -683K
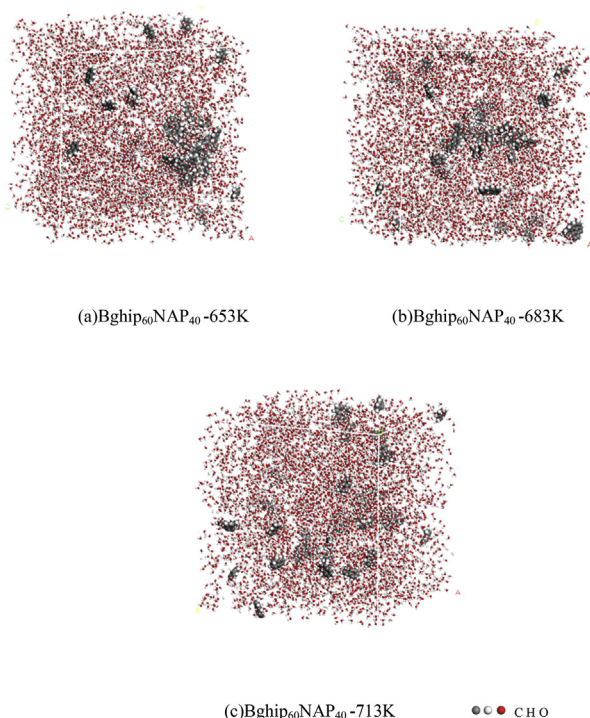
(c)Bghip$_{60}$NAP$_{40}$ -713K　　●●○ ● C H O

Fig. 6 – Solubility of PAHs (Bghip$_{60}$NAP$_{40}$) in SCW/ Hydrogen environment at different temperatures.
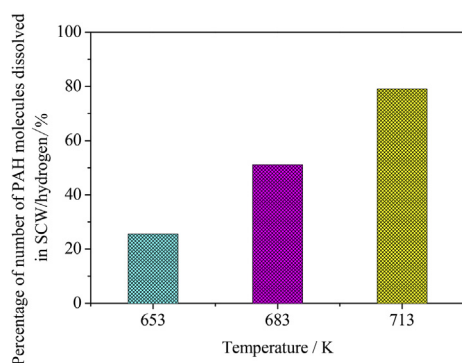

Fig. 7 – Solubility of PAHs (Bghip$_{60}$NAP$_{40}$) in SCW/ Hydrogen environment after 125 ps at various temperatures.

(a)–(c). Relatively, solvation effect was the best at the temperature of 713 K and simultaneously the distribution of PAH molecules in solvent was the most homogeneous. In this case, heavy PAHs were inclined to be successfully dissolved. Besides, at after 125 ps, the miscibility effect of PAHs (Bghip$_{60}$-NAP$_{40}$) droplets with supercritical water/hydrogen was obtained at different temperatures, as indicated in Fig. 7. Even about 80% of PAH molecules in the oil droplet were dissolved into supercritical water/hydrogen environment at a short time of 125 ps when the temperature reached 713 K. The computational results manifested that increasing temperature reinforced the oil droplet solvation in supercritical water/ hydrogen environment.

Conclusions

The solubility behaviors of PAHs in supercritical water/ hydrogen environment were investigated based on molecular dynamics simulation, which was beneficial for understanding the solubility behaviors of oil droplets in the supercritical solvent. The results confirmed that Bghip aggregates were rather stable in supercritical water and hydrogen environment, while NAP aggregates were liable to be rapidly and completely dissolved. Compared with that of pure supercritical water, supercritical water and hydrogen jointly enhanced the dissolution of PAH oil droplets. Furthermore, high water density and high temperature prompted the solvation of PAHs in supercritical water/hydrogen solvent. Approximately 80% of the number of PAH molecules in oil droplet were successfully dissolved in supercritical water/hydrogen environment at a short time of 125 ps and the temperature of 713 K. This work is prospective to provide a theoretical support for the development of complete coal gasification technology in supercritical water for hydrogen production.

Acknowledgements

REFERENCES

[1] Guo L, Jin H. Boiling coal in water: hydrogen production and power generation system with zero net CO$_2$ emission based on coal and supercritical water gasification. Int J Hydrogen Energy 2013;38:12953–67.

[2] Guo L, Jin H, Lu Y. Supercritical water gasification research and development in China. J Supercrit Fluids 2015;96:7151–60.

[3] Yan Q, Lu T, Luo J, Hou Y, Nan X. Exergy cascade release pathways and exergy efficiency analysis for typical indirect coal combustion processes. Combust Theor Model 2019;23:1134–49.

[4] Han L, Zhang R, Bi J, Cheng L. Pyrolysis of coal-tar asphaltene in supercritical water. J Anal Appl Pyrolysis 2011;91:281–7.

[5] Han L, Zhang R, Bi J. Experimental investigation of high temperature coal tar upgrading in supercritical water. Fuel Process Technol 2009;90:292–300.

[6] Cheng L, Zhang R, Bi J. Pyrolysis of a low-rank coal in sub-and supercritical water. Fuel Process Technol 2004;85:921–32.

[7] Liang P, Wang Z, Bi J. Simulation of coal pyrolysis by solid heat carrier in a moving-bed pyrolyzer. Fuel 2008;87:435–42.

[8] Su X, Zhao Y, Zhang R, Bi J. Investigation on degradation of polyethylene to oils in supercritical water. Fuel Process Technol 2004;85:1249–58.

[9] Li K, Zhang R, Bi J. Experimental study on syngas production by co-gasification of coal and biomass in a fluidized bed. Int J Hydrogen Energy 2010;35:2722–6.

[10] Jin H, Guo L, Guo J, Ge Z, Cao C, Lu Y. Study on gasification kinetics of hydrogen production from lignite in supercritical water. Int J Hydrogen Energy 2015;40:7523–9.

[11] Jin H, Lu Y, Liao B, Guo L, Zhang X. Hydrogen production by coal gasification in supercritical water with a fluidized bed reactor. Int J Hydrogen Energy 2010;35:7151–60.

[12] Jin H, Chen B, Zhao X, Cao C. Molecular dynamic simulation of hydrogen production by catalytic gasification of key intermediates of biomass in supercritical water. J Energy Resour Technol 2017;140:041801.

[13] Wu Z, Ou G, Ren Y, Jin H, Guo L. Particle-resolved numerical study of the forced convection heat transfer characteristics of an endothermic-biomass particle placed in supercritical water crossflow. Renewable Energy 2020;158:271–9.

[14] Bai B, Wang W, Jin H. Experimental study on gasification performance of polypropylene (PP) plastics in supercritical water. Energy 2020;191:116527.

[15] Cao C, Bian C, Wang G, Bai B, Xie Y, Jin H. Co-gasification of plastic wastes and soda lignin in supercritical water. Chem Eng J 2020;388:124277.

[16] Zheng M, Li X, Liu J, Wang Z, Gong X, Guo L, Song W. Pyrolysis of liulin coal simulated by GUP-based ReaxFF MD with cheminformatics analysis. Energy Fuel 2014;28:522–34.

[17] Zhang J, Weng X, Han Y, Li W, Cheng J, Gan Z, Gu J. The effect of supercritical water on coal pyrolysis and hydrogen production: a combined ReaxFF and DFT study. Fuel 2013;108:682–90.

[18] Jin HH, Xu B, Li H, Ku X, Fan J. Numerical investigation of coal gasification in supercritical water with the ReaxFF molecular dynamics method. Int J Hydrogen Energy 2018;43:20513–24.

[19] Jin H, Wu Y, Guo L, Su X. Molecular dynamic investigation on hydrogen production by polycyclic aromatic hydrocarbon gasification in supercritical water. Int J Hydrogen Energy 2016;41:3837–43.

[20] Zhang Y, Li J, Wang J, Yang X, Wang B. ReaxFF MDSs-based studies on gasification of glucose in SCW under microwave heating. Int J Hydrogen Energy 2016;41:13390–8.

[21] Liu X, Wang T, He M. Investigation on the condensation process of HFO refrigerants by molecular dynamics simulation. J Mol Liq 2019;288:111034.

[22] Xiang L, Jiang H, Ren F, Chu H, Wang P. Numerical study of the physical and chemical effects of hydrogen addition on laminar premixed combustion characteristics of methane and ethane. Int J Hydrogen Energy 2020;45:20501–14. https://doi.org/10.1016/j.ijhydene.2019.11.040.

[23] Ren F, Xiang L, Chu H, Ya Y, Han W, Nie X. Numerical investigation on the effect of CO_2 and steam for the H_2 intermediate formation and NO_x emission in laminar premixed methane/air flames. Int J Hydrogen Energy 2020;45:3785–94.

[24] Cai S, Hu Z, Li J, Zhang X. Molecular dynamics simulation of infinite dilution diffusivity of carbon dioxide in supercritical water. Int J Mod Phys B 2018;32:1850296.

[25] Cai S, Zhang Y, Hu Z, Zhang X. MD simulation of carbon dioxide diffusion in supercritical water. Bull Sci Technol 2019;2:1–5.

[26] Zhang J, Liu N. Supercritical cyclic stream simulation of wellbore temperature and pressure distribution in Lukeqin oilfield. Int J Heat Technol 2018;36:245–51.

[27] Shvab I, Sadus RJ. Thermophysical properties of supercritical water and bond flexibility. Phys Rev E 2015;92:012124.

[28] Zhao X, Jin H. Investigation of hydrogen diffusion in supercritical water: a molecular dynamics simulation study. Int J Heat Mass Tran 2019;133:718–28.

[29] Zhao X, Jin H, Chen Y, Ge Z. Numerical study of H_2,CH_4,CO,O_2 and CO_2 disffusion in water near the critical point with molecular dynamics simulation. Comput Math Appl 2020. https://doi.org/10.1016/j.camwa.2019.11.012. In press.

[30] Zhao X, Jin H. Correlation for self-diffusion coefficients of H_2,CH_4,CO,O_2 and CO_2 in supercritical water from molecular dynamics simulation. Appl Therm Eng 2020;171:114941.

[31] Svishchev IM, Plugatyr A. Supercritical water oxidation of o-dichlorobenzene: degradation studies and simulation insights. J Supercrit Fluids 2006;37:94–101.

[32] Stubbs JM. Molecular simulations of supercritical fluid systems. J Supercrit Fluids 2015;108:104–22.

[33] Jin H, Liu S, Wei W, Zhang D, Cheng Z. Experimental investigation on hydrogen production by anthracene gasification in supercritical water. Energy Fuel 2015;29:6342–6.

[34] Modell M. Reforming of glucose and wood at the critical condition of water//ASME intersociety conference on environmental systems, san francisco. 1977. p. 8–13.

[35] Chen J, Fan Y, Zhao X, et al. Experimental investigation on gasification characteristic of food waste using supercritical water for combustible gas production: exploring the way to complete gasification. Fuel 2020;263:116735.

[36] Chen J, Fan Y, Jiaqiang E, Cao W, Zhang F, Gong J, Liu G, Xu W. Effects analysis on the reaction kinetic characteristics of the food waste gasification by supercritical water. Fuel 2019;241:94–104.

[37] Fan C, Guo S, Jin H. Numerical study on coal gasification in supercritical water fluidized bed and exploration of complete gasification under mild temperature conditions. Chem Eng Sci 2019;206:134–45.

[38] Bai B, Liu Y, Wang Q, Zou J, Zhang H, Jin H, Li X. Experimental investigation on gasification characteristics of plastic wastes in supercritical water. Renew Energy 2019;135:32–40.

[39] Guo L, Zhao L, Lu Y, et al. Polygeneration technology of hydrogen production from coal gasification in supercritical water. J Eng Thermophys-Rus 2017;3:678–9.

[40] Zhang Y, Li L, Xu P, et al. Hydrogen production through biomass gasification in supercritical water: a review from exergy aspect. Int J Hydrogen Energy 2019;44:15727–36.

[41] Qu H, Gong J, Tan X, Yuan P, Cheng Z, Yuan W. Dissolution of polycyclic aromatic hydrocarbons in subcritical and supercritical water: a molecular dynamics simulation study. Chem Eng Sci 2019;195:958.

[42] Jin H, Ding WJ, Chen B, Bai B, Zhao Q, Cao C. A molecular dynamics simulation investigation on the solubility of polycyclic aromatic hydrocarbons in supercritical water. J Mol Liq 2020;301:112464.

[43] Ding WJ, Jin H, Zhao Q, Chen B, Cao W. Dissolution of polycyclic aromatic hydrocarbons in supercritical water in hydrogen production process: a molecular dynamics simulation study. Int J Hydrogen Energy 2020;45:28062–9. https://doi.org/10.1016/j.ijhydene.2020.02.226.

[44] Wu Z, Ren Y, Ou G, Jin H. Influence of special water properties variation on the heat transfer of supercritical water flow around a sphere. Chem Eng Sci 2020;222:115698.

[45] Sun H. An ab initio force-field optimized for condensed-phase applications overview with details on alkane and benzene compounds. J Phys Chem B 1998;102:7338.

[46] Sun H, Ren P, Fried JR. The COMPASS force field: parameterization and validation for phosphazenes. Comput Theor Polym Sci 1998;8:229–46.

[47] Xin S, Liu Q, Wang K, Chen Y, Yuan P, Cheng Z, Yuan W. Solvation of asphaltenes in supercritical water: a molecular dynamics study. Chem Eng Sci 2016;146:115.

[48] Jin H, Wu Y, Zhu C, Guo L, Huang J. Molecular dynamic investigation on hydrogen production by furfural gasification in supercritical water. Int J Hydrogen Energy 2016;41:1–6.